

Variety in the Coordination Modes of the Ligand Hexakis(pyrazol-1-yl)benzene (Hpzb) to Pd^{II}, Pt^{II} and Cu^I Centres

Ana M. Guerrero,^[a] Félix A. Jalón,^{*[a]} Blanca R. Manzano,^[a] Rosa M. Claramunt,^[b] María Dolores Santa María,^[b] Consuelo Escolástico,^[b] José Elguero,^[c] Ana M. Rodríguez,^[d] Miguel A. Maestro,^[e] and José Mahía^[e]

Keywords: N ligands / Conformational analysis / Palladium / Platinum / Copper / Coordination chemistry

The structure and conformational analysis of eight complexes derived from hexakis(pyrazol-1-yl)benzene (hpzb) have been carried out by means of X-ray crystallography and NMR spectroscopy. The metallic fragments [Pd(C₆F₅)₂], [Pd(η³-2-Me-C₃H₄)⁺], PtCl₂ and Cu(PMe₃)⁺ coordinate with two adjacent pyrazole residues yielding complexes with one, two or three metallic centres. The crystal and molecular structures of [[Pd(C₆F₅)₂]₂(hpzb)], [[Pd(η³-C₄H₇)₂](hpzb)](TfO)₂, [[Cu(PMe₃)₂(hpzb)](BF₄)₂ and [[Pd(η³-C₄H₇)₃(hpzb)](TfO)₃ have been determined. The structure of each of the complexes depends on the fact that the metal

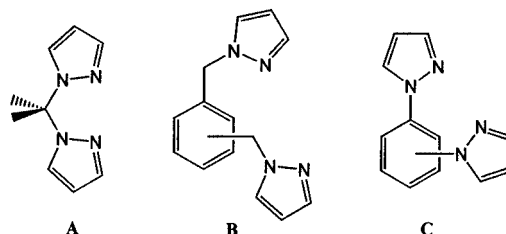
atoms, when two or three are present, prefer to be situated on opposite faces of the benzene ring. Evidence for restricted rotation of the uncoordinated pyrazolyl groups has been found for the free ligand and monometallic derivatives, while free rotation of these groups at room temperature has been observed for the dimetallic complexes. Furthermore, the derivative [[Cu(PMe₃)₂(hpzb)](BF₄)₂ and probably [[Pd(η³-C₄H₇)₂(hpzb)](TfO)₂ exhibit metallotropy on the NMR time scale.

© Wiley-VCH Verlag GmbH, 69451 Weinheim, Germany, 2002)

Introduction

The use of *N*-substituted pyrazoles as ligands is very common, with the three main types of derivatives being polypyrazolylborates (scorpionates), polypyrazolylmethanes **A** and polypyrazolylazines (pyridines, pyrimidines, *s*-triazines, etc.). On the other hand, polypyrazolylbenzenes have seldom been used if one excludes the (pyrazol-1-ylmethyl) derivatives **B** ("coelenterands"),^[1–17] which have structures intermediate between pyrazolylalkanes and (pyrazol-1-yl)benzenes **C** (Scheme 1).

Only five ligands derived from **C** have been used in coordination chemistry: **D**,^[18] **E**,^[19] **F**,^[20] **G**^[21] and **H**^[22–23] (Scheme 2). However, hexakis(pyrazol-1-yl)benzene (hpzb, **1**), which belongs to the "propellene" class of ligands that we have studied systematically,^[24–29] has never previously been used.



Scheme 1

In this paper, we will discuss the coordination chemistry of **1** (hpzb) to different metal atoms with two vacant coordination sites with special emphasis on its conformational aspects. Compound **1**, like other biphenyl-like compounds, has two rotational barriers: the planar barrier, due to steric effects, and the perpendicular one, due to the loss of conjugation. In propellenes the first barrier is much larger than the second one. Therefore, these compounds can be described as having the six azolyl residues librating about the perpendicular conformations, either (*P*) or (*M*) [plus (*P*) or minus (*M*) refers to the sense of rotation, clockwise or counterclockwise, with respect to a perpendicular orientation of the pyrazole and the benzene ring]. We are interested in determining whether in solution, not only in the free ligand but also in the complexes having non-coordinated pyrazolyl groups, free or restricted rotation of these rings exists. Concerning the metallic complexes we were also inter-

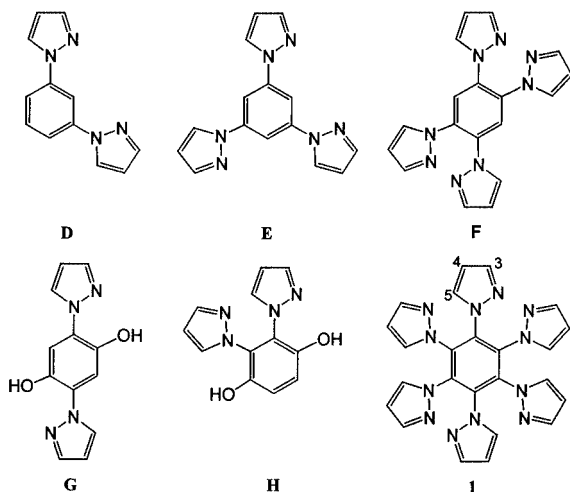
^[a] Departamento de Química Inorgánica, Orgánica y Bioquímica, Universidad de Castilla-La Mancha, Facultad de Químicas, Avda. Camilo J. Cela, 10, 13071 Ciudad Real, Spain
Fax: (internat) + 34-926/295318

^[b] Departamento de Química Orgánica y Biología, Facultad de Ciencias, UNED, Senda del Rey, 9, 28040 Madrid, Spain

^[c] Instituto de Química Médica, CSIC, Juan de la Cierva, 3, 28006 Madrid, Spain

^[d] Departamento de Química Inorgánica, Orgánica y Bioquímica, Universidad de Castilla-La Mancha, E. T. S. de Ingenieros Industriales, Avda. Camilo J. Cela, s/n, 13071 Ciudad Real, Spain

^[e] Servicios Xerais de Apoio á Investigación, Universidade de A Coruña, Campus de A. Zapateira, 15071 A Coruña, Spain



Scheme 2

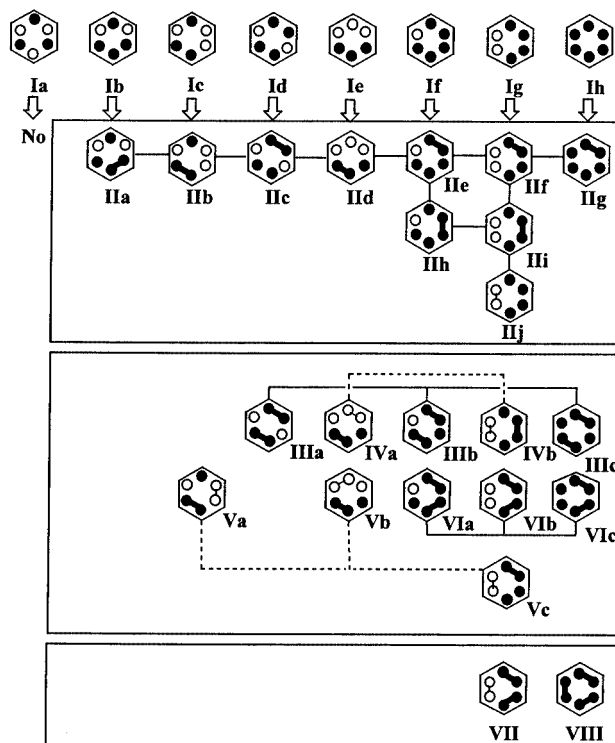
ested in studying the following points: i) The number of metal atoms that is possible to introduce for each hpzb ligand. ii) The disposition of these metal atoms around the six pyrazolyl groups. For example, it was of interest to determine the possibility of having two or more metal atoms at the same side of the benzene plane or two metal atoms bonded to two contiguous pyrazolyl rings. It was foreseeable that the steric requirements of the metallic fragment considering the size and orientation of the ancillary ligands could play an important role in these two points. iii) The presence of fluxional behaviour due to metallotropic shifts and the factors that influence it. iv) Where possible, we also have an interest in analysing the solid-state structure. Interesting points concerning this aspect could be: similarity between complexes of different metals, cooperativity in the orientation of the pyrazolyl groups and correspondence between the solid-state and solution structures. We chose different fragments with late transition metals: $\text{Pd}(\text{C}_6\text{F}_5)_2$, PtCl_2 , $[\text{Pd}(\eta^3\text{-2-Me-C}_3\text{H}_4)]^+$, and Cu^+/PMe_3 . The first two examples with different metals and ancillary ligands of different size were supposed to exhibit a typical square-planar coordination. The allyl fragment had a different orientation of this group that could reduce the symmetry of the derivatives obtained increasing the number of possible isomers. The copper centre was chosen to analyse a case with a different metallic geometry (tetrahedral or trigonal-planar were open possibilities).

Results and Discussion

Conformational Analysis

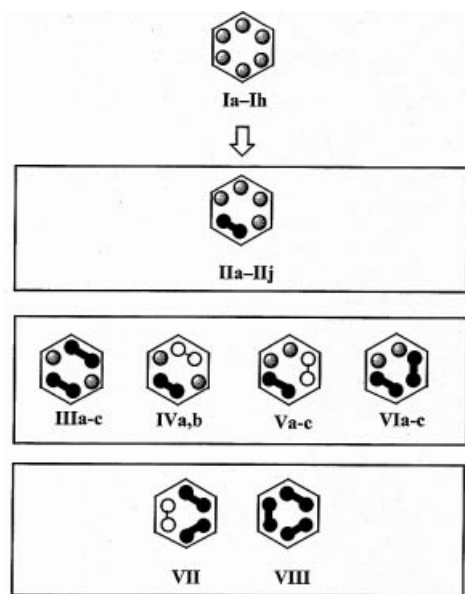
Before describing the synthesis and characterisation of the new derivatives it would be useful to analyse the different isomers that could exist for the ligand and the mono-, di- and trinuclear complexes depending on the relative orientation of the metallic fragments and the uncoordinated pyrazolyl rings.

In derivative **1**, and according to our previous discussion, each pyrazol-1-yl group can adopt two perpendicular conformations depending on whether the N-2 lone pair is *up* (*u*, black dot) or *down* (*d*, white dot). This situation results in the eight isomers **Ia–Ih**, neglecting enantiomerism (**Ic** is chiral), which we have represented at the top of Scheme 3. The hpzb ligand exists in the solid state in two conformations (polymorphism) – *ududud* (**Ia**) and *udduud* (**Ic**).^[25] According to AM1 and SAM calculations, these conformations have torsion angles close to 90° , with the most stable conformer being **Ia** followed, at about 9 kJ mol^{-1} higher, by **Ib**, **Ic** and **Id**, all of which have the same energy.^[28]

Scheme 3. Conformational description of ligand **1** and all possible mono- di- and trimetallic derivatives

The main difficulty concerning the conformation of **1** and its bidentate chelate complexes is to decide between a fixed *up-down* conformation and a free-rotating situation. If we represent a free-rotating pyrazole with a grey dot, we obtain the situation depicted in Scheme 4. In both Schemes we suppose that the metallic fragment does not reduce the symmetry of the complex. It should be noted, however, that free rotation does not signify that all conformations are equally populated. The classifications shown in Scheme 4 are only rigorously true when the *up* and *down* conformations have the same energy.

The formation of a bidentate chelate complex $\kappa^2\text{-N1N2}$ -hpzb (**II**) is not possible for conformation **Ia** but is feasible for all the others, which are related by *u/d* rotations of the uncoordinated pyrazol-1-yl residues (ten conformers **IIa–IIj**). The formation of a second chelation could lead to four different isomers, **III–VI**, two with $\kappa^4\text{-N1N2,N4N5-}$



Scheme 4. Conformational description of ligand **1** and all possible mono-, di- and trimetallic derivatives assuming free rotation of the uncoordinated pyrazoles

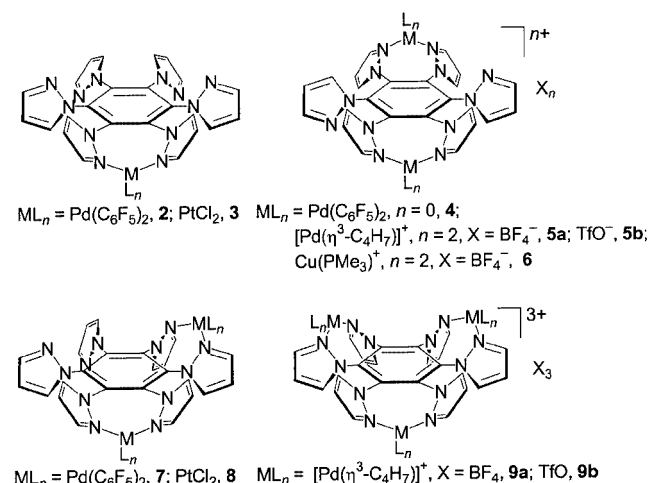
hpzb coordination (three conformers **IIIa–IIIc** and two conformers **IVa, IVb**) and two with κ^4 -*N1N2,N3N4*-hpzb coordination (three conformers **Va–Vc** and three conformers **VIa–VIc**). Finally, the third and final chelation could lead to only two isomers κ^6 -*N1N2,N3N4N5N6*-hpzb (**VII** and **VIII**) without any rotational freedom (they are identical in Schemes 3 and 4).

Synthesis of Complexes

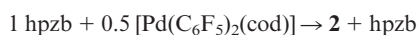
In order to follow the discussion more easily we have included the molecular structures of the new complexes in Scheme 5.

(a) Pd Complexes **2**, **4**, **5**, **7** and **9**

The reaction between hpzb and $[\text{Pd}(\text{C}_6\text{F}_5)_2(\text{cod})]$ led to a mixture of three compounds whose relative proportions depended on the stoichiometry used:



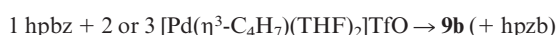
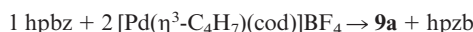
Scheme 5



When **4** and **7** are present in a reaction mixture, their relative ratio is near 50:50. The reaction corresponding to a 1:6 stoichiometry was only carried out in an NMR tube and the attempt to obtain a compound with three Pd centres (analogous to **9**) failed. In order to increase the yield of **2** we used a ratio of 1:0.5. Although **2** was the only metallic complex formed in this reaction we were not able to obtain it in a pure form because it was partially transformed into **4** and **7** in the crystallisation process. Compound **4** (previously separated by crystallisation) was dissolved in $(\text{CD}_3)_2\text{CO}$ and its ^1H NMR spectrum showed an approximately 50:50 mixture of **4** and **7**. This important result shows that structures of type κ^4 -*N1N2,N4N5*-hpzb (**IV**) and κ^4 -*N1N2,N3N4*-hpzb (**V**) rapidly equilibrate in solution.

On the other hand, the reactions with $[\text{Pd}(\eta^3\text{-C}_4\text{H}_7)(\text{THF})_2]\text{TfO}$ or $[\text{Pd}(\eta^3\text{-C}_4\text{H}_7)(\text{cod})]\text{BF}_4$ also depend on the proportions used. In the case of the reaction with $[\text{Pd}(\eta^3\text{-C}_4\text{H}_7)(\text{cod})]\text{BF}_4$, the use of a 1:1 or 1:0.5 stoichiometry gives rise to a solid that could not be characterised as a pure product (see below for NMR in solution). Attempts to crystallise this solid failed. The elemental analyses of the crystallised sample were intermediate between those corresponding to mononuclear and dinuclear complexes.

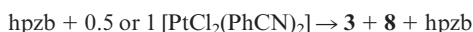
On using 2 or 3 equiv. of the allyl derivatives, the only isolated metallic compound was **9**, which has three palladium centres (**9a** and **9b** differ only in the counteranion: BF_4^- for **9a** and TfO^- for **9b**).



The crystallisation of **9b** led not only to crystals of this trinuclear compound but also to a small amount of crystals of a complex of stoichiometry $[\{\text{Pd}(\eta^3\text{-C}_4\text{H}_7)\}_2\text{-(hpzb)}](\text{TfO})_2$ (**5b**).

(b) Pt Complexes **3** and **8**

The different stoichiometries used correspond to two Equations:

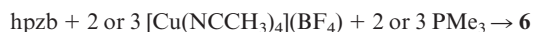


These reactions only reach completion after two weeks at room temperature. On using shorter reaction times the benzonitrile was not completely displaced from the Pt reagent and heating produced decomposition of Pt^{II} into Pt^0 . Mono- and dimetallic derivatives can be separated by chromatography, with the mononuclear complex being eluted

first. We have verified that **8** does not dissociate into **3** and PtCl_2 in an acetone solution.

(c) Cu Complex **6**

This compound was obtained according to the following Equation:



The same derivative was obtained when 2 equiv. of PMe_3 per Cu^+ were used.

The new derivatives are soluble in acetone, THF, chloroform and dichloromethane but are insoluble in pentane, hexane and diethyl ether.

Mass Spectrometry

The main information obtained by this technique concerns the number of metal centres in a given complex. Thus, the MAS-FAB⁺ spectrum of **3** shows peaks at 740 $[\text{M}]^+$, 705 $[\text{M} - \text{Cl}]^+$, 638 $[\text{M} - \text{pz} - \text{Cl}]^+$, 602 $[\text{M} - \text{pz} - 2 \text{ Cl}]^+$ and 475 $[\text{M} - (\text{PtCl}_2)]^+$. The mixture of isomers **4** and **7** did not show the molecular ion peak, only fragments at 1188 $[\text{M} - \text{C}_6\text{F}_5]^+$, 1020 $[\text{M} - 2 (\text{C}_6\text{F}_5)]^+$ and 513 $[\text{M} - \text{pz} - \text{Pd} - 4 (\text{C}_6\text{F}_5)]^+$. Analogously, the most significant fragments in the case of **6** are 841 $[\text{M} - \text{BF}_4]^+$, 613 $[\text{M} - 2 \text{ BF}_4 - \text{Cu}(\text{PMe}_3)]^+$ and 537 $[\text{M} - 2 \text{ BF}_4 - \text{Cu}(\text{PMe}_3) - \text{PMe}_3]^+$, and for **8**, 1006 $[\text{M}]^+$, 933 $[\text{M} - 2 \text{ Cl} - \text{H}]^+$, 740 $[\text{M} - \text{PtCl}_2]^+$, 638 $[\text{M} - \text{pz} - \text{Pt} - 3 \text{ Cl}]^+$, 602 $[\text{M} - \text{Pt} - 4 \text{ Cl}]^+$ and 475 $[\text{M} - 2 (\text{PtCl}_2)]^+$. The trinuclear complex **9b** presents a characteristic spectrum with peaks at 1257 $[\text{M}$

$-\text{TfO}]^+$, 947 $[\text{M} - 2 \text{ TfO} - \{\text{Pd}(\eta^3\text{-C}_4\text{H}_7)\}]^+$ and 635 $[\text{M} - 3 \text{ TfO} - 2 \{\text{Pd}(\eta^3\text{-C}_4\text{H}_7)\}]$.

X-ray Structural Characterisation of Complexes **4**, **5b**, **6** and **9b**

A number of problems were encountered in the NMR spectroscopic study, including the difficulty in differentiating between the coordinated and noncoordinated pyrazoles. Hence, it is appropriate to discuss the crystallographic study first.

Crystallographic and selected structural data are compiled in Tables 1 and 2, respectively. ORTEP plots of the structures are shown in Figures 1–4. The bad quality of the crystals and the failure of obtaining new crystals made it impossible to obtain an adequate refinement for **5b**. However, the data indicate unambiguously the position of the two palladium fragments.

Pd or Cu atoms are in an approximately square- or trigonal-planar environment, respectively. The bite angle of hpzb for the Cu complex **6** is small (93.14°) for a trigonal-planar disposition, which indicates a marked difference in the angles of the coordination plane.

The molecular structures for complexes **4** (Figure 1), **5b** (Figure 2) and **6** (Figure 3) show the two metallic units in a coordination type **IV** ($\kappa^4\text{-N1N2,N4N5-hpzb}$) with one metal atom *up* and the other *down*. The existence, in these derivatives, of a crystallographic inversion centre in the geometric central point of the molecule ensures that the uncoordinated pyrazole rings are oppositely oriented with respect to the benzene plane (*up* and *down*). As a consequence, conformer **IVa** is the only one present in the solid state for

Table 1. Crystal data and structure refinement for **4**, **6** and **9b** ($R_1 = \Sigma||F_o| - |F_c||/\Sigma|F_o|$; $wR_2 = \{\Sigma [w(F_o^2 - F_c^2)^2]/\Sigma[w(F_o^2)^2]\}^{0.5}$)

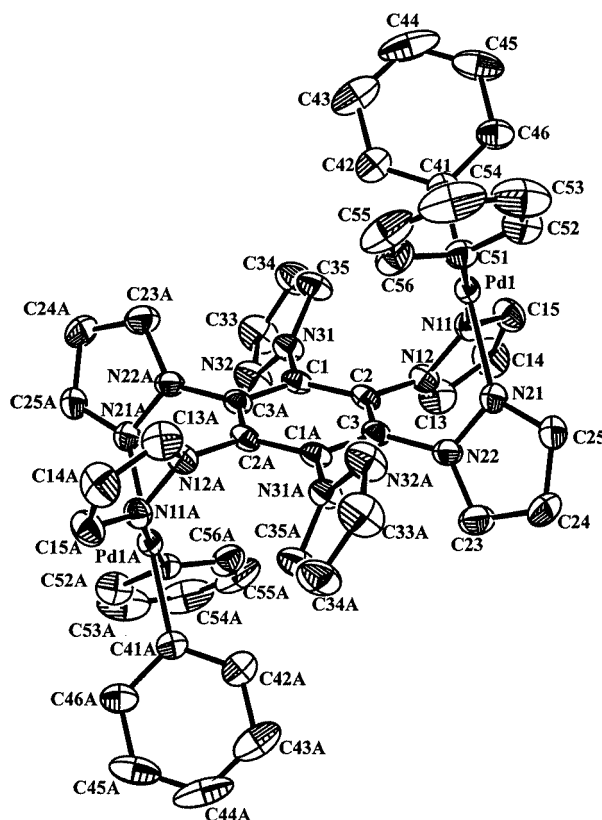
| | 4 | 6 | 9b |
|---|---|--|--|
| Empirical formula | $\text{C}_{48}\text{H}_{18}\text{F}_{20}\text{N}_{12}\text{Pd}_2$ | $\text{C}_{30}\text{H}_{36}\text{B}_2\text{Cu}_2\text{F}_8\text{N}_{12}\text{P}_2$ | $\text{C}_{38}\text{H}_{40}\text{F}_9\text{N}_{12}\text{O}_9\text{Pd}_3\text{S}_3$ |
| Formula mass | 1355.54 | 927.35 | 1395.20 |
| Temperature [K] | 293(2) | 173(2) | 298(2) |
| Wavelength [Å] | 0.71073 | 0.71073 | 0.71073 |
| Crystal system | triclinic | monoclinic | orthorhombic |
| Space group | $P\bar{1}$ | $P2_1/n$ | $Pnma$ |
| <i>a</i> [Å] | 11.082(6) | 11.5148(11) | 28.404(5) |
| <i>b</i> [Å] | 13.359(5) | 13.2698(13) | 17.494(3) |
| <i>c</i> [Å] | 18.481(2) | 13.4157(13) | 11.498(2) |
| α [°] | 71.55(1) | 90 | 90 |
| β [°] | 80.58(2) | 108.625(2) | 90 |
| γ [°] | 72.32(4) | 90 | 90 |
| Volume [Å ³] | 2465.9(16) | 1942.6(3) | 5713.5(19) |
| <i>Z</i> , calculated density [g/cm ³] | 2, 1.826 | 2, 1.585 | 4, 1.622 |
| Absorption coefficient [cm ⁻¹] | 0.856 | 1.257 | 1.129 |
| <i>F</i> (000) | 1324 | 940 | 2764 |
| Crystal size [mm] | 0.4 × 0.3 × 0.1 | 0.40 × 0.35 × 0.30 | 0.40 × 0.35 × 0.30 |
| Limiting indices | 0 ≤ <i>h</i> ≤ 14 −16 ≤ <i>k</i> ≤ 17 −23 ≤ <i>l</i> ≤ 24 | −15 ≤ <i>h</i> ≤ 15 −17 ≤ <i>k</i> ≤ 17 −17 ≤ <i>l</i> ≤ 12 | −33 ≤ <i>h</i> ≤ 32 −20 ≤ <i>k</i> ≤ 19 −12 ≤ <i>l</i> ≤ 13 |
| Reflections collected/unique | 11897/11897 [<i>R</i> (int) = 0] | 13692/4823 [<i>R</i> (int) = 0.0739] | 29203/5048 [<i>R</i> (int) = 0.1567] |
| Data/restraints/parameters | 11897/0/739 | 4823/0/325 | 5048/0/311 |
| Goodness-of-fit on <i>F</i> ² | 0.942 | 0.942 | 0.907 |
| Final <i>R</i> indices [<i>I</i> > 2σ(<i>I</i>)] | <i>R</i> 1 = 0.0421, <i>wR</i> 2 = 0.0672 | <i>R</i> 1 = 0.0475, <i>wR</i> 2 = 0.0864 | <i>R</i> 1 = 0.0886, <i>wR</i> 2 = 0.2458 |
| Largest diff. peak/hole [eÅ ⁻³] | 0.758/−0.705 | 0.488/−0.437 | 1.42/−0.773 |

Table 2. Selected bond lengths [\AA] and angles [$^\circ$] for complexes **4**, **6** and **9b**

| | | | |
|-------------------|-----------|-------------------|-----------|
| 4 | | | |
| Pd(1)–C(41) | 1.998(5) | C(41)–Pd(1)–N(11) | 94.1(2) |
| Pd(1)–C(51) | 1.983(5) | C(51)–Pd(1)–N(21) | 94.3(2) |
| Pd(1)–N(11) | 2.080(4) | C(41)–Pd(1)–N(21) | 179.3(2) |
| Pd(1)–N(21) | 2.089(4) | N(11)–Pd(1)–N(21) | 85.2(1) |
| C(1)–C(2) | 1.401(6) | C(3A)–C(1)–C(2) | 119.3(4) |
| C(1)–N(31) | 1.414(5) | C(3A)–C(1)–N(31) | 120.4(4) |
| C(1)–C(3A) | 1.390(6) | C(2)–C(1)–N(31) | 120.2(4) |
| C(2)–C(3) | 1.394(6) | C(3)–C(2)–C(1) | 120.1(4) |
| C(2)–N(12) | 1.414(5) | C(3)–C(2)–N(12) | 120.4(4) |
| C(3)–N(22) | 1.412(5) | C(1)–C(2)–N(12) | 119.5(4) |
| C(51)–Pd(1)–C(41) | 86.4(2) | C(1A)–C(3)–C(2) | 120.5(4) |
| C(51)–Pd(1)–N(11) | 177.1(2) | C(1A)–C(3)–N(22) | 119.3(4) |
| 6 | | | |
| Cu(1)–N(2) | 2.004(2) | C(4)–C(5) | 1.378(4) |
| Cu(1)–N(4) | 2.044(3) | C(4)–C(6A) | 1.396(4) |
| Cu(1)–P(1) | 2.1756(9) | C(5)–C(6) | 1.391(4) |
| C(4)–C(5) | 1.378(4) | N(2)–Cu(1)–N(4) | 93.14(9) |
| C(4)–C(6A) | 1.396(4) | N(2)–Cu(1)–P(1) | 143.62(7) |
| C(5)–C(6) | 1.391(4) | N(4)–Cu(1)–P(1) | 122.64(7) |
| N(1)–C(5) | 1.426(3) | C(5)–C(4)–C(6A) | 120.6(3) |
| N(3)–C(4) | 1.422(4) | C(4)–C(5)–C(6) | 119.8(2) |
| N(5)–N(6) | 1.362(3) | C(5)–C(6)–C(4A) | 119.6(3) |
| 9b | | | |
| Pd(1)–C(18) | 2.15(2) | C(2)–C(3) | 1.38(2) |
| Pd(1)–C(17) | 2.13(2) | C(3)–C(3A) | 1.42(2) |
| Pd(1)–C(16) | 2.11(2) | C(1)–C(1A) | 1.42(2) |
| Pd(1)–N(2) | 2.12(1) | C(1)–C(2) | 1.38(2) |
| Pd(1)–N(4) | 2.12(1) | N(2)–Pd(1)–N(4) | 89.9(4) |
| Pd(2)–C(13) | 2.11(2) | N(6)–Pd(2)–N(6A) | 88.4(7) |
| Pd(2)–C(14) | 2.14(2) | C(2)–C(3)–C(3A) | 119.2(6) |
| Pd(2)–N(6) | 2.12(1) | C(2)–C(1)–C(1A) | 119.0(6) |
| | | C(1)–C(2)–C(3) | 122(1) |

these dinuclear compounds. This is not the only similarity between the three structures: (i) Firstly, the uncoordinated pyrazole rings, which are in *para* positions with respect to one another, adopt a conformational orientation suitable for minimising the steric hindrance with the neighbouring rings, in such a way that the six pyrazole rings are distributed in two sets: three twisted (*P*) and three twisted (*M*). (ii) The dihedral planes of the pyrazole rings and the benzene rings are very similar (58 – 68° , Table 2), not only in **4** and **6** but also in one of the polymorphic forms of the free hpzb ligand.^[25] (iii) The N–Pd–N bite angles do not differ greatly (84 – 93°). (iv) As a consequence of the two preceding statements the central cores, including the hpzb and the metallic centres, are practically superimposable for these three structures.

The structure of complex **4** (Figure 1) shows the two $\text{Pd}(\text{C}_6\text{F}_5)_2$ fragments oriented *up* and *down* in relation to the benzene ring and pointing in towards the core of the molecule. Considering this orientation and the considerable

Figure 1. ORTEP view with atomic numbering of **4** (30% probability ellipsoids); the F atoms have been omitted for clarity

volume of this metallic fragment, it is very unlikely that three metallic units of this type could be coordinated with the same hpzb ligand and this hypothesis is in accordance with the experimental observations.

The trimetallic derivative $[\{\text{Pd}(\eta^3\text{-C}_4\text{H}_7)\}_3(\text{hpzb})](\text{TfO})_3$ (**9b**) (Figure 4) has a structure of type $\kappa^6\text{-N1N2,N3N4,N5N6}$ -hpzb with two (allyl)palladium units on the opposite side to that of the third, with respect to the plane of the benzene ring (isomer type **VII**). The three methylallyl groups are oriented away from the molecule. This orientation, in conjunction with the considerably smaller volume of the (allyl)palladium unit with respect to the other groups used in this work, allows the coexistence of two vicinal metallic centres on the same side of the benzene ring. The small size of the crystals obtained precluded a final refinement of the structure, but a general overview of the backbone is possible. Bite and torsional angles of the pyrazole rings are in the range found for structures described previously. This structure is also preserved in solution (*vide infra*).

In summary, when more than one metal atom is present they prefer to be situated on opposite faces of the benzene ring. A reasonable extension to complexes **7** and **8** is that they adopt a **Va**, **Vb** or **Vc** disposition.

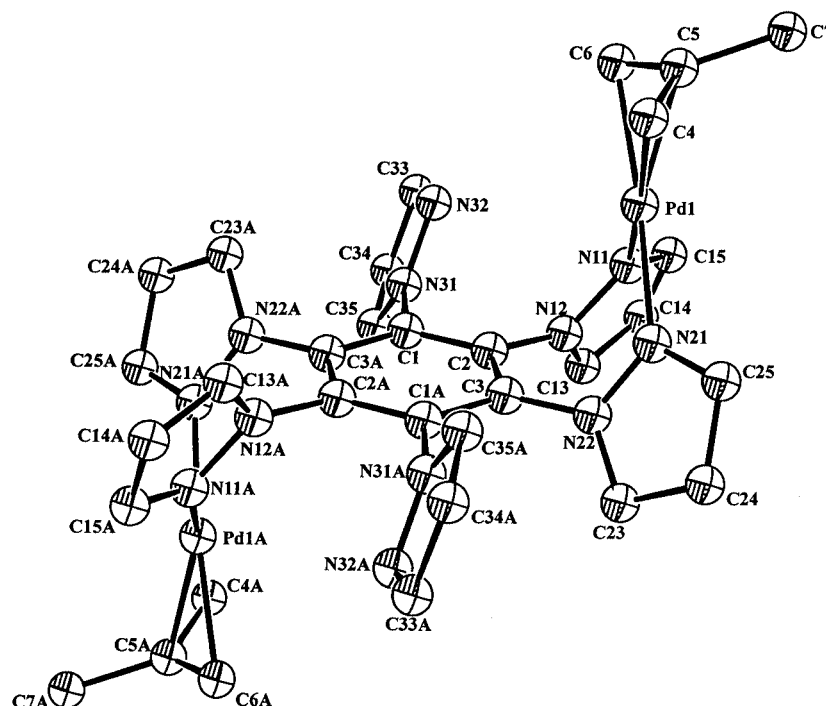


Figure 2. ORTEP view with atomic numbering of the cation of **5b** (30% probability ellipsoids)

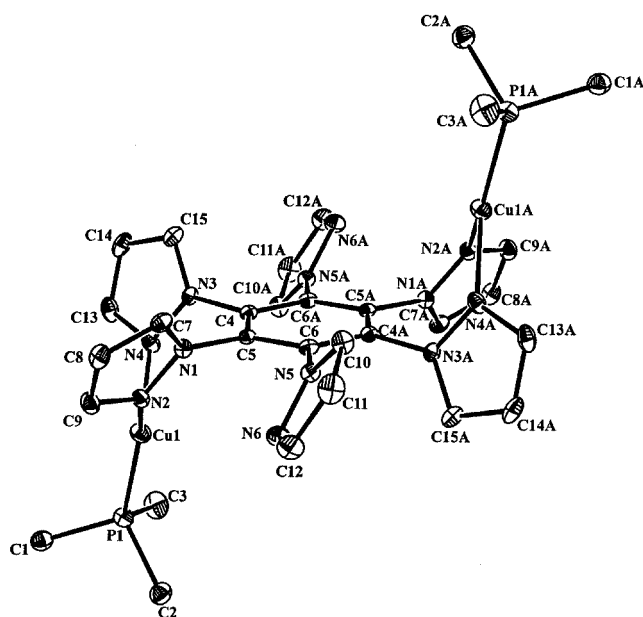


Figure 3. ORTEP view with atomic numbering of the cation of **6** (30% probability ellipsoids)

NMR Spectroscopic Studies in Solution

Before a discussion on the NMR spectroscopic data is undertaken, it is useful to classify the different conformations of Schemes 3 and 4 according to their symmetry point groups and the expected number of different pyrazole rings (see Table 3). There is a one-to-one correspondence between the point group and the number of pyrazole rings with the exception of the C_s case where, depending on whether the symmetry plane lies between two *ortho*-pyrazole rings or

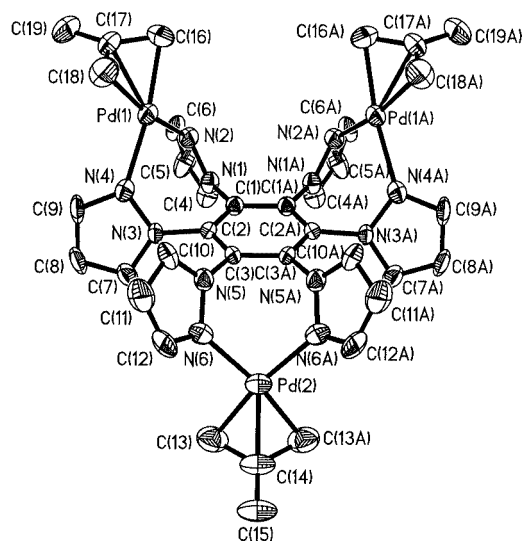


Figure 4. ORTEP view with atomic numbering of the cation of **9b** (30% probability ellipsoids)

through two *para*-pyrazole rings, the number of expected signals is 1:1:1 or 1:2:2:1, respectively.

Free Ligand hpzb (1)

This ligand can exist in the eight perpendicular conformations (**1a–1h**) shown in Scheme 3. When the ^1H NMR spectrum was recorded in CDCl_3 (4 mg/0.6 mL), signals of only one type of pyrazole ring could be observed (Table 4). This could correspond to the highly symmetric *ududud* (**1a**) or *uuuuuu* (**1h**) conformations or the average conformation

Table 3. Point groups and patterns of the signals in NMR spectra (see Schemes 3 and 4)

| Conformation | Point group | No of pz rings | Conformation | Point group | No. of pz rings |
|-------------------------------------|-------------|----------------|------------------|-------------|-----------------|
| Ia | D_{3d} | 1 | Ia–Ih | D_{6h} | 1 |
| Ib, If | C_s | 1:2:2:1 | | | |
| Ic | C_2 | 1:1:1 | | | |
| Id | C_{2v} | 1:2 | | | |
| Ie | C_{2h} | 1:2 | | | |
| Ig | C_s | 1:1:1 | | | |
| Ih | C_{6v} | 1 | | | |
| Ila, Iib, Ild, Iie, Iif, Iih | C_1 | 1:1:1:1:1:1 | Ila–Iij | C_s | 1:1:1 |
| Iic, Iig, Iii, Iij | C_s | 1:1:1 | | | |
| IIla, IIlc | C_{2v} | 1:2 | IIla–IIlc | C_{2v} | 1:2 |
| IIlb | C_s | 1:2:2:1 | | | |
| IVa | C_i | 1:1:1 | IVa/IVb | C_{2h} | 1:2 |
| IVb | C_s | 1:1:1 | | | |
| Va, Vb | C_2 | 1:1:1 | Va–Vc | C_2 | 1:1:1 |
| Vc | C_1 | 1:1:1:1:1:1 | | | |
| VIa | C_1 | 1:1:1:1:1:1 | VIa–VIc | C_s | 1:1:1 |
| VIb, VIc | C_s | 1:1:1 | | | |
| VII | C_s | 1:1:1 | VII | C_s | 1:1:1 |
| VIII | C_{3v} | 1 | VIII | C_{3v} | 1 |

Ia–Ih. Conformation **Ih** can be excluded on the basis of its very high energy.^[25,28] The difficult problem remains in deciding between the static (except for librations) conformation **Ia** or the dynamic one **Ia–Ih**.

Table 4. ^1H NMR chemical shifts and ^1H – ^1H coupling constants of the free ligand hpzb (**1**) (δ in ppm and J in Hz)

| Solvent | Conformer | Intensity | 3-H | 4-H | 5-H |
|----------------------------|-----------------------------|-----------|------------------|------------------|------------------|
| CDCl_3 | <i>ududud</i> (Ia) | 1 | 7.41 | 6.12 | 7.25 |
| | | | $^4J_{35} = 0.6$ | $^3J_{34} = 1.7$ | $^3J_{45} = 2.4$ |
| CD_3COCD_3 | <i>ududud</i> (Ia) | 1 | 7.32 | 6.11 | 7.43 |
| | | | $^4J_{35} = 0.6$ | $^3J_{34} = 1.7$ | $^3J_{45} = 2.5$ |
| | <i>uuduud</i> (Id) | 1 | 7.63 | 6.41 | 7.73 |
| | | | $^4J_{35} = 0.6$ | $^3J_{34} = 1.8$ | $^3J_{45} = 2.5$ |
| | | 2 | 7.88 | 6.65 | 8.13 |
| | | | $^4J_{35} = 0.6$ | $^3J_{34} = 1.8$ | $^3J_{45} = 2.5$ |

When the spectrum of this compound was recorded in $(\text{CD}_3)_2\text{CO}$, in which the compound is rather insoluble, one or two isomers were observed depending on the concentration. In a very dilute solution (2 mg/0.6 mL) signals of only one kind of pyrazole ring was observed, as was the case in CDCl_3 . However, in a more concentrated solution (saturated, i.e. about 6 mg/0.6 mL), two isomers were observed (the signals are narrow in all cases). The most abundant isomer (60%) corresponds to that already described above. The minor isomer (40%), however, has two kinds of pyrazole rings in a 1:2 ratio. First conclusion: the average **Ia–Ih** dynamic system shown in Scheme 4 can definitely be ruled out at room temperature on the NMR time-scale. A low-temperature ^1H NMR spectrum (193 K), in which signal splitting was not observed, also confirmed this statement. Consequently, the major isomer is **Ia** and the signals of the minor isomer, according to Table 3, should correspond either to conformer **Id** or **Ie**. Since the second conformer is much higher in energy,^[25] we conclude that the minor iso-

mer is the *uuduud* compound **Id**. It should be noted that this isomer has also been observed in a small amount in other hexakis(azol-1-yl)benzenes.^[28]

The following discussion refers to the new complexes **2–9**.

(a) ^1H NMR Spectroscopy

The ^1H – ^1H coupling constants, which are higher for 5-H/4-H than for 4-H/3-H, were used to differentiate the corresponding signals. In cases where different pyrazolyl groups were observed for a specific compound, COSY experiments allowed the signals belonging to the same pyrazole ring to be identified (Table 5).

For the mononuclear complexes **2** and **3**, three different types of pyrazole rings were evident, a situation in agreement with conformations **Iic**, **Iig**, **Iii** or **Iij** in Scheme 3 or with the dynamic situations **Ila–Iij** in Scheme 4 (see Table 3). In the low-temperature spectrum (193 K) of **2**, evidence for splitting of the signals was not observed. On extrapolating the result to **3**, we propose a static situation for both derivatives, similar to that found in the free ligand. If the orientation of two contiguous free pyrazolyl groups towards the same side of the benzene ring is considered less stable (see ref.^[25] for energy calculations for the free ligand), **2** and **3** should have the structure of conformer **Iic**.

Three different situations have been found in the NMR spectra of the dinuclear compounds: (i) In complex **4** two kinds of pyrazole signals were observed in a ratio of two (coordinated) to one (noncoordinated). The existence of conformers **IIla** or **IIlc** or the dynamic equilibria **IIla/IIlb/IIlc** or **IVa/IVb** are consistent with the experimental data. However, according to the X-ray results the steric hindrance that will arise from the orientation of two $\text{Pd}(\text{C}_6\text{F}_5)_2$ fragments on the same side of the benzene ring allows us to rule out conformers of type **III** and, consequently, the equilibrium **IVa/IVb** is proposed. Moreover, the dynamic situ-

Table 5. ^1H NMR spectroscopic data for complexes **2–4** and **6–9**

| Compd. ^[a] | 3-H' | 4-H' | 5-H' | 3-H'' | 4-H'' | 5-H'' | 3-H''' | 4-H''' | 5-H''' | Other groups |
|--|---------------------------|---------|--------------------------|--------------------------|---------|--------------------------|--------------------------|---------|--------------------------|--|
| 2 | 7.44 d* $J_{34} = 2.1$ | 6.15 dd | 7.14 d $J_{45} = 2.7$ | 7.42*d $J_{34} = 1.8$ | 6.21 dd | 7.45 d $J_{45} = 2.8$ | 7.83 d $J_{34} = 1.7$ | 6.38 dd | 7.75 d $J_{45} = 2.7$ | – |
| 3 | 7.50 d $J_{34} = 1.9$ | 6.15 pt | 7.68 d $J_{45} = 2.6$ | 7.37 d $J_{34} = 1.9$ | 6.25 pt | 7.40 d $J_{45} = 2.5$ | 8.05 d $J_{34} = 1.9$ | 6.47 pt | 7.66 d $J_{45} = 2.9$ | – |
| 4 | 7.97 d $J_{34} = 2.1$ | 6.50m | 7.75 d $J_{45} = 2.8$ | 7.99 d $J_{34} = 2.1$ | 6.50m | 7.52 $J_{45} = 2.8$ | 7.99 d $J_{34} = 2.1$ | 6.50 m | 7.52 $J_{45} = 2.8$ | – |
| 6 | 7.66 d $J_{34} = 1.9$ | 6.46 pt | 8.16 d $J_{45} = 2.9$ | 7.66 d | 6.46 pt | 8.16 d | 7.66 d | 6.46 pt | 8.16 d | [1.42 br. s (PMe ₃)] |
| 7 | 7.31 d $J_{34} = 1.6$ | 6.24 dd | 6.94 d $J_{45} = 2.4$ | 7.47 d $J_{34} = 1.8$ | 6.28 dd | 7.15 d $J_{45} = 2.4$ | 8.00 d $J_{34} = 2.3$ | 6.44 dd | 7.13 d $J_{45} = 2.8$ | – |
| 8 | 7.53 d $J_{34} = 1.9$ | 6.61 pt | 7.23 d $J_{45} = 2.4$ | 8.10 d $J_{34} = 2.5$ | 6.52 pt | 7.52 m ^[b] | 8.15 d $J_{34} = 2.2$ | 6.38 pt | 7.69 d $J_{45} = 2.9$ | – |
| $\eta^3\text{-C}_4\text{H}_7$ (2-Me-allyl) | | | | | | | | | | |
| 9b | 8.15 d $J_{34} = 2.1$ | 6.60 pt | 8.74 d $J_{45} = 2.4$ | 8.22 d $J_{34} = 1.9$ | 6.52m | 8.02 d $J_{45} = 2.7$ | 8.11 d $J_{34} = 2.1$ | 6.52m | 7.66 d $J_{45} = 2.6$ | 2.38 s (3 H) 3.91 br. s (2 H) 3.70 br. s (4 H) 3.60 br. s (2 H) 3.71 br. s (2 H) 3.79 br. s (2 H) |
| 9b ^[c] | 8.36m | 6.73 pt | 8.77 d | 8.48 d | 6.68 pt | 7.91 d | 8.36 m | 6.64 pt | 7.66 m | 2.35 s (6 H) 2.31 br. s (9 H) 3.60 br. s (2 H) 4.38 br. s (6 H) |
| 9a ^[d] | 8.26 d $J_{34} = 2.0$ | 6.71 pt | 8.48 d $J_{45} = 2.6$ | 8.37 d $J_{34} = 2.0$ | 6.63 pt | 7.72 d $J_{45} = 3.0$ | 8.27 d $J_{34} = 2.0$ | 6.60 pt | 7.48 d $J_{45} = 2.8$ | 2.35 s (6 H) 2.38 s (3 H) 3.81 s (2 H) 3.49 s (2 H) 3.66 s (2 H) 4.32 s (2 H) 4.36 s (2 H) 4.39 s (2 H) |

^[a] $T = 293$ K if not indicated; δ in ppm; J in Hz.; solvent = $(\text{CD}_3)_2\text{CO}$. See formula **1** in Scheme 2 for numbering. Unless specified, the signals are singlets; d = doublet, br. s = broad singlet, m = multiplet, pt = pseudotriplet. ^[b] Signal partially overlapped. ^[c] $T = 183$ K. ^[d] $T = 213$ K. The signals marked with * have not been unequivocally assigned to one specific pyrazole ring.

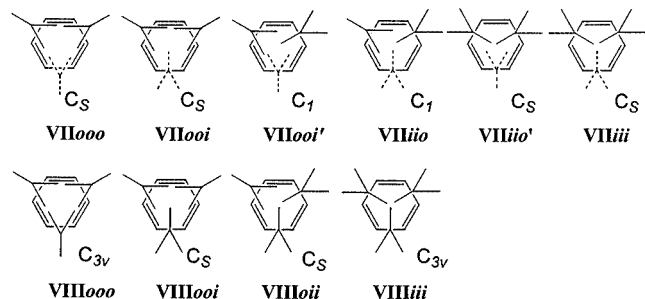
ation is confirmed by a low-temperature NMR spectrum (193 K). The resonances of the coordinated pyrazole rings are broad at 233 K and a splitting is finally observed at lower temperatures. Although the resonances of the noncoordinated pyrazole rings are less sensitive to temperature, the corresponding 5-H signal also broadens and splits at low temperature. (ii) In complexes **7** and **8** three different pyrazole rings in a 1:1:1 ratio are observed; two for each pair of coordinated pyrazole rings and a third for the non-coordinated system. If we again exclude conformers that have the two metallic fragments on the same side of the benzene plane (**VIb**, **VIc** and **VIa**/**VIb**/**VIc**) the possible conformers would be: **IVa**, **IVb**, **Va**, **Vb** or the equilibrium **Va**/**Vb**/**Vc** (see Table 3). In the case of complex **7**, conformers **IVa** and **IVb** are not possible because the equilibrium **IVa**/**IVb** is the only possibility for **4** and is observed separately from **7**. Splitting of some signals is observed in both derivatives at low temperature. Consequently, the equilibrium **Va**/**Vb**/**Vc** is proposed for **7** and **8** at room temperature. (iii) In **6**, other dynamic processes must operate in addition to pyrazolyl rotation. Only broad signals due to one type of pyrazole ring are observed, some of which remain broad even at 203 K. A metallotropic process by exchange of the metal atoms between the pyrazole rings must take place and averaged signals are observed.

For the solid obtained in the reaction between hpzb and $[\text{Pd}(\eta^3\text{-C}_4\text{H}_7)(\text{cod})]\text{BF}_4$ (1:0.5 or 1:1 ratio), one broad signal for 4-H and two broad and overlapped signals for 3-H and 5-H are observed at room temperature. The spectrum at 323 K exhibits narrower signals and a very complex spectrum is observed at low temperature (193 K). We propose

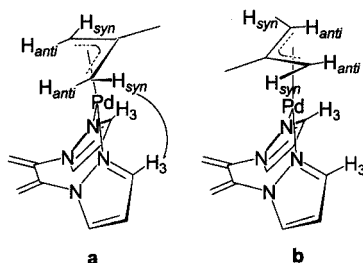
that a mixture of complex **5a** (analogous to **5b** with a BF_4^- anion), adopting some of the possible structural configurations, (**III–VI** of Scheme 3) and free hpzb are present in equilibrium at room temperature by a metallotropic process. The concomitant presence of a mononuclear complex cannot be excluded.

A particularly interesting case is that of complex **9**. Three kinds of pyrazole rings are observed in a 1:1:1 ratio. Although some signal overlap seems to occur in the allylic region, at low temperature three separate H_{anti} signals (1:1:1 ratio) are observed. It is necessary to consider that the methyl group of the 2-methylallyl group can point inside (*i*) or outside (*o*) the benzene ring. This reduction in symmetry of the (allyl)Pd fragment when compared with that of the previously described MX_n groups, makes the symmetry considerations in Table 3 not strictly applicable in this case. Scheme 6 shows representations of the isomers derived from structures **VII** (six isomers) and **VIII** (four isomers). The symmetry point group is indicated in each case. When the symmetry is C_{3v} , one type of pyrazole ring is expected, but six types would occur if the symmetry is C_1 and three if it is C_s . Consequently, the experimental data only fit with the conformers of C_s symmetry. Several NOE experiments were carried out at room temperature (**9a** and **9b**): upon irradiation of H_{anti} (*anti*) an NOE effect was observed with H_{syn} (*syn*) and when H_{syn} was irradiated the NOE effect was observed not only on H_{anti} but also on the three signals of 3-H (closer to H_{syn} than 5-H) (Scheme 7). This confirms the previous assignment of these pyrazolic protons but, more importantly, indicates that the three allyl groups have an outside orientation. Consequently, if we consider the con-

formers of C_s symmetry, only conformer **VIIooo** fits with the NOE data and we propose this structure for complex **9** in solution. The fact that interchange of the (allyl)palladium fragments between the pyrazolyl groups is not observed, in contrast to **5**, could be due to the absence of free pyrazolyl rings in this derivative.



Scheme 6. Representation of the isomers corresponding to structures **VII** and **VIII**



Scheme 7. **a** and **b** represent the outside and inside orientations, respectively, of the allyl group; only in **a** the NOE observed in compound **9** (indicated with an arrow between H_{syn} and 3-H of the pyrazolyl group) is possible

Conclusions concerning the possible conformers in solution for complexes **2–9** are collected in Table 6. The conformation of the molecule in the solid state is also included in cases where it is known. The first conclusion is that structures found in the solid state are consistent with those in solution in the cases of complex **9** (one conformer) and with one of the possible conformations of **4–6**. A static behaviour has been found in the free ligand and the monometallic derivatives while in the dimetallic complexes free rotation of the uncoordinated pyrazolyl groups is observed at room temperature. A slowing down of this rotation is observed at low temperature. In derivatives **5** and **6** the occurrence of other fluxional processes has prevented the study of this phenomenon.

(b) ^{13}C NMR Spectroscopy

The most significant information from the data in Table 7 regards the number of different pyrazole rings observed that

Table 6. Conformation of complexes **2–9** in the solid state and in $(\text{CD}_3)_2\text{CO}$ solution

| Compd. | Solid state | | Solution | | |
|---------------|-------------|------------|--------------|--------------------------------|-----------------|
| | Class | Structure | Class | Structure rigid ^[a] | Structure free |
| 2 (Pd) | II | — | II | <i>IIc, IIg, Ili, IIj</i> | — |
| 3 (Pt) | II | — | II | <i>IIc, IIg, Ili, IIj</i> | — |
| 4 (Pd) | IV | IVa | IV | — | IVa/IVb |
| 5 (Pd) | IV | IVa | IV | [fluxional] | — |
| 6 (Cu) | IV | IVa | IV | [fluxional] | — |
| 7 (Pd) | — | — | V | — | Va/Vb/Vc |
| 8 (Pt) | — | — | IV, V | — | Va/Vb/Vc |
| 9 (Pd) | VII | VII | VII | VII | — |

^[a] Structure numbers in italics are considered to be the most stable.

Table 7. $^{13}\text{C}\{^1\text{H}\}$ NMR spectroscopic data for hpzb (**1**) ligand and complexes **2–4** and **6–9**

| Compd. ^[a] | C-3' | C-4' | C-5' | Benzene | Other groups | | |
|----------------------------------|----------------------|----------------------|----------------------|-------------|--|---------------------|---------------------|
| hpzb (1) ^[b] | 141.5 | 107.2 | 132.3 | 136.6 | — | | |
| | 142.3 | 108.0 | 129.2 | 132.4 | — | | |
| | 142.6 | 108.6 | 133.3 | 142.9 | | | |
| 3 | 144.8 | 109.5 | 137.2 | n.o. | | | |
| | 142.4 | 107.9 | 133.6 | n.o. | — | | |
| | 144.0 | 110.1 | 134.4 | | | | |
| 4 | 147.0 | 111.8 | 138.1 | | | | |
| | 145.8 ^[c] | 111.6 ^[c] | 136.4 ^[c] | n.o. | — | | |
| | 146.0 | 111.4 | 137.4 | | | | |
| 6 | 143.4 br. s | 108.7 br. s | 134.5 br. s | 137.7 br. s | [17.5 br. s, PMe ₃] | | |
| 7 | 143.9 | 109.9 | 132.0 | n.o. | — | | |
| | 144.4 | 110.6 | 132.7 | | | | |
| | 146.8 | 112.4 | 135.8 | | | | |
| 8 | 143.3 | 109.3 | 132.7 | n.o. | — | | |
| | 146.4 | 111.2 | 137.2 | | | | |
| | 146.7 | 112.5 | 137.8 | | | | |
| 9b | | | | | η ³ -C ₄ H ₇ (2-Me-allyl) | | |
| | | | | | —C= | CH ₂ | CH ₃ |
| | 147.9 | 109.5 | 136.7 | 137.4 | 137.4 | 63.2 ^[c] | 23.3 ^[c] |
| | 147.9 | 110.7 | 138.4 | 137.7 | 137.8 ^[c] | 64.2 | 23.4 |
| | 148.2 | 111.0 | 140.3 | 138.1 | | | |

^[a] $T = 293\text{ K}$; δ in ppm; solvent = $(\text{CD}_3)_2\text{CO}$. See formula **1** of Scheme 2 for numbering. ^[b] CDCl_3 . ^[c] These peaks have an intensity twice that of the others. For **9b**, the CF_3SO_3^- signal appears at $\delta = 121.7$ (q, $^1J_{\text{C,F}} = 319\text{ Hz}$) ppm.

Table 8. ^{19}F NMR chemical shifts (ppm from CFCl_3) and ^{19}F - ^{19}F coupling constants (Hz) for **2**, **4** and **7** in $(\text{CD}_3)_2\text{CO}$

| Compd. | F_{ortho} | F_{meta} | F_{para} |
|----------|--|--|--|
| 2 | −119.8/−117 (br. m, 4 F) | −166.6 (br. m, 4 F) | −164.2 (t, 2 F) $^3J(F_p-F_m) = 18.3$ |
| 4 | −115.0 (d, 8 F) $^3J(F_o-F_m) = 30.5$ | −168.8 (m, 8 F) | −167.2 (t, 4 F) $^3J(F_p-F_m) = 18.3$ |
| 7 | −115.2 (d, 4 F) $^3J(F_o-F_m) = 30.6$ −118.0 (d, 4 F) $^3J(F_o-F_m) = 30.5$ | −165.8 (br. m, 4 F) −166.4 (br. m, 4 F) | −163.3 (t, 2 F) $^3J(F_p-F_m) = 18.3$ −163.9 (t, 2 F) $^3J(F_p-F_m) = 18.3$ |

are in agreement with those presented in Table 5: **3** (1:1:1), **4** (1:2), **6** (fluxional behaviour), **7**, **8** and **9** (1:1:1).

(c) ^{19}F NMR Spectroscopy

In accordance with the expected symmetry, and as deduced from the number of F_{para} signals observed, one kind of C_6F_5 ring exists in compounds **2** and **4** and two kinds (1:1 ratio) in derivative **7**. These belong to C_6F_5 groups either close to the other metal centre or close to a noncoordinated pyrazole ring. The F_{ortho} or F_{meta} signals are broad in some cases, indicating a certain degree of restricted rotation (Table 8).

Conclusions

After the reaction of the ligand hpzb (**1**) with different metallic fragments $\{\text{Pd}(\text{C}_6\text{F}_5)_2\}$, $[\text{Pd}(\eta^3\text{-2-Me-C}_3\text{H}_4)]^+$, PtCl_2 and $\text{Cu}(\text{PMe}_3)^+$ we have synthesised new mono-, di- and trinuclear derivatives. We have carried out an analysis of the complex energy hypersurface that these complexes present, reporting many examples which describe fairly well its multidimensional aspect. The incorporation of three metallic centres was only possible with the smaller group $[\text{Pd}(\eta^3\text{-C}_4\text{H}_7)]^+$, a clear indication of the influence of steric effects. We have found that the metallic fragments, when two or three are present, prefer to be situated on opposite faces of the benzene ring. As far as the fluxionality of the compounds is concerned, we observed two types of behaviour on the NMR spectroscopic time-scale: metalotropic processes and rotation of the uncoordinated pyrazolyl groups. The former process was found in the dimetallic derivatives **5** and **6** with (allyl)palladium and $\text{Cu}(\text{PMe}_3)$ fragments, respectively. The second process described was the free rotation of the uncoordinated pyrazolyl groups that was found in the rest of the dimetallic complexes (**4**, **7** and **8**) at room temperature, although the process slows down at low temperature. Restricted rotation was observed in the monometallic derivatives and the free ligand even at room temperature. For complex **9**, where all the pyrazole rings are involved in coordination to the metal centre, a fluxional process is not observed. Finally, on a much slower time-scale, when the Pd^{II} derivative **4** was dissolved in $(\text{CD}_3)_2\text{CO}$ an approximately 50:50 mixture of **4** and **7** was obtained. This fact shows that structures of type $\kappa^4\text{-N1N2,N4N5-}$

hpzb (**IV**) and $\kappa^4\text{-N1N2,N3N4-}$ hpzb (**V**) equilibrate in solution (isomerism). The X-ray structure of three dimetallic derivatives (**4**, **5b** and **6**) and the trinuclear derivative **9b** was undertaken. All the structures with two metallic centres were of the type $\kappa^4\text{-N1N2,N4N5-}$ hpzb (**IV**) and the central core (hpzh ligand and metal centre) was near superimposable. Cooperative rearrangement of the pyrazolyl rings to minimize the steric hindrance was found in these dinuclear derivatives. When allyl ligands were present, they had the methyl group pointing away from the molecule. In all cases, the structures determined in the solid state were in accordance with the situations found in solution.

Experimental Section

General Comments: All manipulations were carried out under dry oxygen-free nitrogen using standard Schlenk techniques. Solvents were distilled from the appropriate drying agents and degassed before use. The ligand hexakis(pyrazol-1-yl)benzene (hpzb, **1**) has been previously described.^[25,27] $[\text{Pd}(\text{C}_6\text{F}_5)_2(\text{cod})]$ (cod = 1,5-cyclooctadiene) was synthesised as described in the literature for similar complexes.^[30] $[\text{PtCl}_2(\text{PhCN})_2]$ was prepared according to Kharasch,^[31] $[\text{Pd}(\eta^3\text{-C}_4\text{H}_7)(\mu\text{-Cl})_2]$ according to Wilkinson^[32] and $[\text{Cu}(\text{CH}_3\text{CN})_4](\text{BF}_4)$ according to Kubas.^[33] Elemental analyses were performed with a Perkin–Elmer 240 B microanalyser. IR spectra were recorded in Nujol mulls with a Perkin–Elmer 883 (4000–200 cm^{-1} range) spectrophotometer. ^1H , ^{13}C , and ^{19}F NMR spectra were recorded with a Varian Unity 300 spectrometer using, unless specified, $(\text{CD}_3)_2\text{CO}$ as solvent. Standard experimental conditions were employed.^[34,35] Mass spectra (position of the peaks in Da) were recorded with a VG Autospec spectrometer (University of Zaragoza) using the FAB^+ technique and *m*-nitrobenzyl alcohol as matrix.

Preparation of Compounds

(a) $[\text{Pd}(\text{C}_6\text{F}_5)_2(\text{hpzb})]$ (2**) and $[\{\text{Pd}(\text{C}_6\text{F}_5)_2\}_2(\text{hpzb})]$ (**4** and **7**):** We have carried out the reaction using different metal/ligand stoichiometries (0.5, 1, 2 or 3). Different mixtures (white colour) of the three isomers were obtained accordingly with the results specified in the previous section. Here we report the experiment with a 1:3 stoichiometry. $\text{Pd}(\text{C}_6\text{F}_5)_2(\text{cod})$ (242 mg, 0.42 mmol) was added to a solution of hpzb (70.0 mg, 0.14 mmol) in THF (20 mL). The mixture was stirred for 7 h. The solution was then concentrated to near dryness and pentane (10 mL) was added, a white solid precipitated that was filtered, washed with pentane to eliminate the cod and dried. Yield of **4** + **7**: 80% (155 mg). IR: $\tilde{\nu} = 1639\text{--}1627$, $1510\text{--}1500$, $1070\text{--}1054$, $975\text{--}950$, 798 , 796 and 787 cm^{-1} (C_6F_5).

Although **2** was the only metallic complex (in a mixture with hpzb) formed in the reaction with a metal/ligand ratio of 0.5, we were not able to obtain it in a pure form because in the crystallisation process, it was partially transformed into **4** and **7**. Compound **7** was never isolated, only a mixture of **4** and **7** without **2** was obtained. **4** + **7**: $C_{48}H_{18}F_{20}N_{12}Pd_2 \cdot 1/2C_4H_8O$ (1399.62): calcd. C 42.91, H 1.58, N 12.01; found C 43.13, H 1.53, N 11.75. From the mixture of the 1:3 reaction, a pure sample of **4** was obtained when preparing crystals for X-ray diffraction by diffusion with acetone/hexane.

(b) [(PtCl₂)(hpzb)] (3) and [(PtCl₂)₂(hpzb)] (8): 1 equiv. of PtCl₂(PhCN)₂ (74.6 mg, 0.16 mmol) under nitrogen was added to a solution of hpzb (75.0 mg, 0.16 mmol) in dry acetone (20 mL). The mixture was stirred at room temperature for 2 weeks. The solution was concentrated to near dryness and pentane (10 mL) was added, a yellow solid precipitated that was filtered, washed with pentane and dried. The mixture of **3** and **8** were separated by flash chromatography (silica gel; eluent: methanol) and a small amount of both derivatives was obtained. IR: $\tilde{\nu}$ = 347 cm⁻¹ [ν(Pt–Cl)] for both complexes. **3**: $C_{24}H_{18}Cl_2N_{12}Pt$ (740.49): calcd. C 38.93, H 2.45, N 22.70; found C 38.79, H 2.37, N 22.60.

(c) [(PtCl₂)₂(hpzb)] (8): The synthesis was carried out as described above, except that 2 equiv. of PtCl₂(PhCN)₂ {hpzb (37.9 mg), [PtCl₂(PhCN)₂] (75.5 mg)} were used. In this way a pure sample of **8** was obtained after washing the yellow precipitate with pentane. Yield: 86% (68.0 mg). $C_{24}H_{18}Cl_4N_{12}Pt_2$ (1006.48): calcd. C 29.63, H 1.80, N 16.61; found C 29.17, H 1.91, N 16.36. The use of a 1:3 stoichiometry again affords **8**.

(d) [{Pd(η³-C₄H₇)₂(hpzb)](X)₂ (5) and [{Pd(η³-C₄H₇)₃(hpzb)](X)₃ (9) [X = BF₄⁻ (a), TfO⁻ (b)]: We have carried out the reaction with different ligand/metal stoichiometries and using the solvate [Pd(η³-C₄H₇)(THF)₂](TfO) (TfO: triflate, trifluoromethylsulfonate) or the derivative [Pd(η³-C₄H₇)(cod)]BF₄ as metallic precursors (see discussion of the results). Here we report on the experiment with a 1:3 stoichiometry and the solvate precursor. First, a solution of [Pd(η³-C₄H₇)(THF)₂](TfO) was prepared from [Pd(η³-C₄H₇)(μ-Cl)]₂ (87.1 mg, 0.22 mmol) and AgTfO (113 mg, 0.44 mmol) in freshly distilled THF (20 mL). The mixture was stirred for 2 h and protected from light. The solution was filtered through Celite to eliminate AgCl. The addition to this solution of the ligand (70.0 mg, 0.15 mmol) produced a white precipitate and the suspension was stirred for 3 h. The solid was filtered and washed with diethyl ether. The solid was crystallised in acetone/pentane to obtain crystals of **9b**. IR: $\tilde{\nu}$ = 835 [ν(C–CH₃) of the allyl group], 1282, 1165, 1031, 767 and 638 cm⁻¹ (TfO⁻ anion). Yield: 75% (155 mg). $C_{39}H_{39}F_9N_{12}O_9Pd_3S_3$ (1406.22): calcd. C 33.31, H 2.79, N 11.95; found C 33.01, H 2.08, N 11.53. When the crystallisation was carried out in acetonitrile/diethyl ether, crystals of [{Pd(η³-C₄H₇)₂(hpzb)](TfO)₂ (**5b**) were obtained.

(e) [{Cu(PMe₃)₂(hpzb)](BF₄)₂ (6): PMe₃ (0.30 mmol, 0.30 mL, 1 M solution in toluene) was added to a solution of [Cu(NCCH₃)₄](BF₄) (94.4 mg, 0.30 mmol) in dry acetone (30 mL). The colourless solution was stirred for 15 min, then hpzb (71.1 mg, 0.15 mmol) was added and the resulting pale yellow solution was stirred for 4 h, concentrated to dryness and washed with diethyl ether. A yellow solid was obtained. Yield: 81% (113 mg). $C_{30}H_{36}B_2Cu_2F_8N_{12}P_2$ (927.36): calcd. C 38.84, H 3.91, N 18.11; found C 38.22, H 4.02, N 18.07. IR: $\tilde{\nu}$ = 1084 and 520 cm⁻¹ (BF₄⁻ anion). The crystals for X-ray diffraction were obtained by crystallisation in dichloromethane/pentane.

X-ray Data Collection, Structure Determination, and Refinement of Complexes 4, 5b, 6 and 9b:^[36] Crystal data and basic information

about the data collection and structure refinement are listed in Table 1. The diffraction experiments were carried out with a CAD4-MACH3 diffractometer (**4** and **5b**) with ω-2θ scan technique to a maximum value of 56° and a Bruker Smart CCD based diffractometer (**6** and **9b**) by using graphite-monochromated Mo-K_α radiation with ψ-ω scan technique (**6** and **9b**). For **4**, the asymmetric unit comprises two half molecules, and for **5b** and **6**, one independent half molecule. Data were corrected for Lorentz and polarisation effects and absorption correction was made for **6** and **9b**. The structures were solved by direct methods (SHELXS)^[37] and refined first isotropically by full-matrix least squares using SHELXL-97^[38] program and then anisotropically by blocked full-matrix least squares for all the non-hydrogen atoms. The hydrogen atoms were included in calculated positions and refined “riding” on their parent carbon atoms.

Acknowledgments

We gratefully acknowledge financial support from the Dirección General de Enseñanza Superior e Investigaciones Científicas, DGES, Spain (Grant N. PB98-0315) and from the DGI/MCyT/ (project number BQU2000-0252).

- [1] W.-K. Chang, S. C. Sheu, G.-H. Lee, Y. Wang, T.-I. Ho, Y.-C. Lin, *J. Chem. Soc., Dalton Trans.* **1993**, 687–694.
- [2] W.-K. Chang, G.-H. Lee, Y. Wang, T.-I. Ho, Y. O. Su, Y.-C. Lin, *Inorg. Chim. Acta* **1994**, 223, 139–144.
- [3] C. M. Hartshorn, P. J. Steel, *Austr. J. Chem.* **1995**, 48, 1587–1599.
- [4] C. M. Hartshorn, P. J. Steel, *Angew. Chem. Int. Ed. Engl.* **1996**, 35, 2655–2657; *Angew. Chem.* **1996**, 108, 2818–2820.
- [5] C. M. Hartshorn, P. J. Steel, *Chem. Commun.* **1997**, 541–542.
- [6] C. M. Hartshorn, P. J. Steel, *Austr. J. Chem.* **1997**, 50, 1195–1198.
- [7] W.-K. Chang, G.-H. Lee, Y. Wang, Y. O. Su, T.-I. Ho, Y.-C. Lin, *J. Coord. Chem.* **1997**, 42, 253–260.
- [8] J. Chen, D. M. L. Goodgame, S. Menzer, D. J. Williams, *Polyhedron* **1997**, 16, 1679–1687.
- [9] J. S. Fleming, K. L. V. Mann, C.-A. Carraz, E. Psillakis, J. C. Jeffery, J. A. McCleverty, M. D. Ward, *Angew. Chem. Int. Ed.* **1998**, 37, 1279–1281. *Angew. Chem.* **1998**, 110, 1325–1328.
- [10] J. S. Fleming, K. L. V. Mann, S. M. Couchman, J. C. Jeffery, J. A. McCleverty, M. D. Ward, *J. Chem. Soc., Dalton Trans.* **1998**, 2047–2052.
- [11] C. M. Hartshorn, P. J. Steel, *Organometallics* **1998**, 17, 3487–3496.
- [12] B. Therrien, T. R. Ward, *Angew. Chem. Int. Ed.* **1999**, 38, 405–408. *Angew. Chem.* **1999**, 111, 418–421.
- [13] J. Chin, C. Walsdorff, B. Stranix, J. Oh, H. J. Chung, S.-M. Park, K. Kim, *Angew. Chem. Int. Ed.* **1999**, 38, 2756–2759. *Angew. Chem.* **1999**, 111, 2923–2926.
- [14] N. Fatin-Rouge, E. Toth, D. Perret, R. H. Backer, A. E. Merbach, J.-C. G. Bünzli, *J. Am. Chem. Soc.* **2000**, 122, 10810–10820.
- [15] C. M. Hartshorn, P. J. Steel, *Inorg. Chem. Commun.* **2000**, 3, 476–481.
- [16] A. J. Canty, J. Patel, B. W. Skelton, A. H. White, *J. Organomet. Chem.* **2000**, 607, 194–202.
- [17] H. P. Dijkstra, M. D. Meijer, J. Patel, R. Kreiter, G. P. M. van Klink, M. Lutz, A. L. Spek, A. J. Canty, G. van Koten, *Organometallics* **2001**, 20, 3159–3168.
- [18] A. J. Canty, R. T. Honeyman, B. W. Skelton, A. H. White, *J. Organomet. Chem.* **1990**, 389, 277–288.
- [19] M. Loi, M. W. Hosseini, A. Jouaiti, A. De Cian, J. Fischer, *Eur. J. Inorg. Chem.* **1999**, 1981–1985.
- [20] A. Jouaiti, M. Loi, M. W. Hosseini, A. De Cian, *Chem. Commun.* **2000**, 2085–2086.

- [21] P. Cornago, C. Escolástico, M. D. Santa María, R. M. Claramunt, D. Carmona, M. Esteban, L. A. Oro, C. Foces-Foces, A. L. Llamas-Saiz, J. Elguero, *J. Organomet. Chem.* **1994**, *467*, 293–301.
- [22] [22a] T. E. Keyes, P. M. Jayaweera, J. J. McGarvey, J. G. Vos, *J. Chem. Soc., Dalton Trans.* **1997**, 1627–1632. [22b] T. E. Keyes, R. J. Forster, P. M. Jayaweera, C. G. Coates, J. J. McGarvey, J. G. Vos, *Inorg. Chem.* **1998**, *37*, 5925–5932.
- [23] A. M. Bond, F. Marken, C. T. Williams, D. A. Beattie, T. E. Keyes, R. J. Forster, J. G. Vos, *J. Phys. Chem. B* **2000**, *104*, 1977–1983.
- [24] C. Foces-Foces, A. L. Llamas-Saiz, R. M. Claramunt, N. Jagerovic, M. L. Jimeno, J. Elguero, *J. Chem. Soc., Perkin Trans. 2* **1995**, 1359–1371.
- [25] C. Foces-Foces, A. L. Llamas-Saiz, C. Escolástico, R. M. Claramunt, J. Elguero, *J. Phys. Org. Chem.* **1996**, *9*, 137–144.
- [26] C. Foces-Foces, C. Fernández-Castaño, R. M. Claramunt, C. Escolástico, J. Elguero, *J. Phys. Org. Chem.* **1996**, *9*, 717–727.
- [27] C. Foces-Foces, A. L. Llamas-Saiz, C. C. Fernández-Castaño, R. M. Claramunt, C. Escolástico, J. L. Lavandera, M. D. Santa-María, M. L. Jimeno, J. Elguero, *J. Chem. Soc., Perkin Trans. 2* **1997**, 2173–2177.
- [28] R. M. Claramunt, J. Elguero, C. Escolástico, C. Fernández-Castaño, C. Foces-Foces, A. L. Llamas-Saiz, M. D. Santa María, *Targets Heterocycl. Syst.* **1997**, *1*, 1–56.
- [29] C. Foces-Foces, C. Fernández-Castaño, R. M. Claramunt, C. Escolástico, J. Elguero, *J. Incl. Phenom. Macrocycl. Chem.* **1999**, *33*, 169–189.
- [30] P. Espinet, J. M. Martínez-de Ilarduya, C. Pérez-Briso, A. L. Casado, M. A. Alonso, *J. Organomet. Chem.* **1998**, *551*, 9–20.
- [31] M. S. Kharasch, R. C. Sailer, F. R. Mayo, *J. Am. Chem. Soc.* **1938**, *60*, 882–887.
- [32] W. T. Dent, R. Long, G. Wilkinson, *J. Chem. Soc.* **1964**, 1585–1588.
- [33] G. J. Kubas, *Inorg. Synth.* **1979**, *19*, 90–92.
- [34] F. Gómez-de la Torre, A. de la Hoz, F. A. Jalón, B. R. Manzano, A. Otero, A. M. Rodríguez, M. C. Rodríguez-Pérez, A. Echevarría, J. Elguero, *Inorg. Chem.* **1998**, *37*, 6606–6614.
- [35] F. Gómez-de la Torre, A. de la Hoz, F. A. Jalón, B. R. Manzano, A. M. Rodríguez, J. Elguero, M. Martínez-Ripoll, *Inorg. Chem.* **2000**, *39*, 1152–1162.
- [36] CCDC-185478 ([Pd (C₆F₅)₂]₂(hpzb)], -185479 ([{Pd(η³-2-Me-C₃H₄)₂(hpzb)](TfO)₂], -185480 ([Cu(PMe₃)₂(hpzb)](BF₄)₂ and -185481 ([{Pd(η³-2-Me-C₃H₄)₃(hpzb)](TfO)₃] contain the supplementary crystallographic data for this paper. These data can be obtained free of charge at www.ccdc.cam.ac.uk/conts/retrieving.html or from the Cambridge Crystallographic Data Centre, 12, Union Road, Cambridge CB2 1EZ, UK [Fax: (internat.) + 44-1223/336-033; E-mail: deposit@ccdc.cam.ac.uk].
- [37] G. M. Sheldrick, *SHELXS-97*, University of Göttingen, Göttingen, Germany, **1990**.
- [38] G. M. Sheldrick, *SHELXL-97, Program for the Refinement of Crystals Structures from Diffraction Data*, University of Göttingen, Göttingen, Germany, **1997**.

Received May 13, 2002
[I02252]